


Enhancing the charging performance of quantum batteries with the work medium of an entangled coupled-cavity array

Hong-Bing Ma,¹ Kai Xu ,^{1,*} Hong-Guo Li,¹ Zong-Guo Li,¹ and Han-Jie Zhu²

¹*Tianjin Key Laboratory of Quantum Optics and Intelligent Photonics, School of Science, Tianjin University of Technology, Tianjin 300384, China*

²*Beijing National Laboratory for Condensed Matter Physics, Institute of Physics, Chinese Academy of Sciences, Beijing 100190, China*



(Received 26 May 2024; accepted 2 August 2024; published 21 August 2024)

Although entanglement is considered as a crucial resource for quantum information processing, it is still unknown whether the presence of quantum entanglement in the working medium can enhance the charging performance of a quantum battery (QB). Here, we address this problem by considering a QB with working medium consisted of an entangled coupled-cavity array. We show that the optimal charging performance of the QB is achieved in the two-cavity case when cavities are initially in a maximum entangled state without cavity couplings. We then extend our discussion to multicavity case. It is demonstrated that the charging power of the QB under an entangled coupled-cavity array can be further enhanced by increasing the number of cavities. Our findings reveal the advantage of an entangled working medium in enhancing the charging performance of a QB, and therefore, contribute to the experimental realization of quantum batteries with excellent performance.

DOI: [10.1103/PhysRevA.110.022433](https://doi.org/10.1103/PhysRevA.110.022433)

I. INTRODUCTION

The quantum battery (QB) [1–8], capable of storing and extracting energy, has emerged as a popular research topic, offering valuable insights into thermodynamics at the quantum scale. Recently, significant research efforts have been dedicated to enhancing the performance of the QB, both theoretically [9–40] and experimentally [41–43]. Theoretical researchers have constructed different QB models based on various quantum systems [21–31]. They have examined various facets of the QB, including stored energy, average charging power, and ergotropy, through the lens of their respective models [32–40]. Strategies to augment the charging performance of a QB have also been expounded. For instance, the authors have illustrated that the QB can be fully charged using a harmonic driving field [29]. It has been found that the single-cavity-mediated charging process for a QB can significantly improve the energy transfer efficiency compared to both the qubit-mediated charging process and the direct charging process of the QB [32]. In experiments, the charging process of the QB has been explored using superconducting qutrit systems [41], optical systems [42], and organic micro-cavity systems [43].

In addition, researchers have discovered that exploiting quantum phenomena, such as quantum coherence and entanglement, can improve the charging performance (i.e., stored energy, average charging power, and extractable work) of quantum batteries [44–48]. It has been shown that when the battery and charger are initially in a product pure state and no energy can be initially extracted from the battery, quantum coherence in the battery or the battery-charger entanglement is

a necessary resource for generating nonzero extractable work during the charging process [47]. The extractable work of the QB can be improved by exploiting the charger-charger entanglement [48]. Furthermore, a recent experiment showed that the energy conversion efficiency of quantum engines using entangled atoms as the working medium can be significantly improved [49]. Based on this experiment, an interesting question arises: Can entangled working media improve the charging performance of the QB? If so, this could provide assistance for the realization of optimal QB experimentally using an entangled working medium.

In this paper, we investigate the impact of an entangled coupled-cavity array on the charging performance of a QB when it serves as a working medium. We demonstrate that the QB achieves optimal charging performance in the two-cavity case when the cavities are initially in a maximum entangled state without cavity couplings. We separately explain the reason for the impact of initial cavity-cavity entanglement, as well as the intercavity coupling, on the QB's charging performance by examining the changes in the QB-charger entanglement and the frequency detuning between the QB and charger and the cavity fields during the charging process. Subsequently, we extend our model to the multicavity case. Consistent with the two-cavity scenario, the achievement of optimal battery charging performance requires no coupling between the multiple cavities, regardless of whether the multiple cavities are initially in an entangled state or a separable state. Moreover, it has been shown that under an entangled coupled-cavity array, the average charging power of a QB can be further enhanced by increasing the number of cavities.

This paper is organized as follows. In Sec. II, physical quantities (i.e., the stored energy, the average charging power, and ergotropy) to evaluate the charging performance of QB are introduced. In Sec. III, the conditions for obtaining the

*Contact author: kxu19930314@163.com

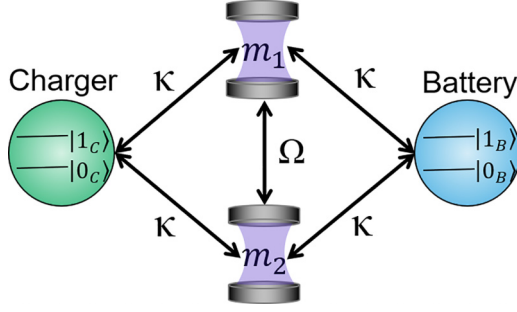


FIG. 1. Schematic representation of the two entangled coupled-cavity that mediate energy transfer between the QB and the charger.

optimal charging performance of a QB are explored when two entangled coupled-cavity mediate the charging process of a QB. When multiple cavities mediate the QB charging process, how to obtain the optimal charging performance is investigated in Sec. IV. Finally, a simple conclusion of this paper is given in Sec. V.

II. QUANTUM BATTERY

To assess the performance of a quantum battery (QB), the average charging power, the ergotropy, and the energy stored in a given time interval are introduced. By considering a time interval $[0, \tau]$ during which the interaction occurs, the energy stored of the QB at time τ is given by [5,32,46]

$$E_B(\tau) = \text{Tr}\{\rho_B(\tau)H_B\} - \text{Tr}\{\rho_B(0)H_B\}, \quad (1)$$

where $\rho_B(\tau)$ is the reduced density matrix of the QB at time τ , H_B is the Hamiltonian of the QB.

The average charging power of a QB can be defined as [9]

$$P_B(\tau) = E_B(\tau)/\tau. \quad (2)$$

To quantify the maximum energy that can be extracted from a QB at the end of the charging process through cyclic unitary operations, the ergotropy is introduced as [50–52]

$$W_B(\tau) = \text{Tr}\{\rho_B(\tau)H_B\} - \text{Tr}\{\sigma_{\rho_B}H_B\}, \quad (3)$$

where σ_{ρ_B} is the passive state of $\rho_B(\tau)$ [53]. The passive states σ_{ρ_B} are defined as those states that do not allow for work extraction in a cyclic (unitary) process.

Then to assess the conditions for acquiring the optimal QB, we concentrate on the maximum energy storage $E_{\max} = \max_{\tau}[E_B(\tau)]$, maximum average charging power $P_{\max} = \max_{\tau}[P_B(\tau)]$, and maximum ergotropy $W_{\max} = \max_{\tau}[W_B(\tau)]$. In the subsequent analysis, we utilize $E_B(\tau)$ (E_{\max}), $P_B(\tau)$ (P_{\max}), and $W_B(\tau)$ (W_{\max}) to examine the effect of the entangled coupled-cavity on the charging performance of the QB. Larger values of $E_B(\tau)$, $P_B(\tau)$, and $W_B(\tau)$ are required to achieve the optimal charging performance of a QB.

III. TWO ENTANGLED COUPLED-CAVITY MEDIATED THE CHARGING PROCESS OF A QB

We first consider the scenario where two entangled coupled cavities mediate the charging process of a QB, as shown in

Fig. 1. We focus on the effects of initial cavity-cavity entanglement and the coupling between the cavities on the QB's charging performance. Under the rotating-wave approximation (RWA), the total Hamiltonian can be written as (with $\hbar = 1$)

$$H = H_0 + f(t)H_I, \quad (4)$$

where

$$H_0 = \frac{\omega}{2}\sigma_z^B + \frac{\omega}{2}\sigma_z^C + \omega a_1^\dagger a_1 + \omega a_2^\dagger a_2, \quad (5)$$

$$H_I = \kappa(\sigma_+^B a_1 + \sigma_-^B a_1^\dagger + \sigma_+^C a_2 + \sigma_-^C a_2^\dagger) + \kappa(\sigma_+^C a_1 + \sigma_-^C a_1^\dagger + \sigma_+^B a_2 + \sigma_-^B a_2^\dagger) + \Omega(a_1^\dagger a_2 + a_1 a_2^\dagger). \quad (6)$$

Here H_0 refers to the free Hamiltonian of the total system. The interaction Hamiltonian H_I respectively describes the interaction between the QB and the cavities with a coupling strength of κ , the interaction between the charger and the cavities with a coupling strength of κ , and the interaction between the cavities with a coupling strength of Ω . The interaction Hamiltonian can also be tuned on (off) by manipulating $f(t)$. The parameter $f(t)$ is set to 1 during the charging period $[0, \tau]$ and 0 otherwise, serving as a classical parameter that represents the external control applied to the system. Before $t = 0$, there is no interaction among the charger, the cavities, and a QB, hence preventing any energy exchange from occurring. In the time interval $0 < t < \tau$, the coupled Hamiltonian is turned on and the four subsystems are coupled together to facilitate the transfer of energy from the charger, through the cavities, and then to the QB. The energy stored in the battery is preserved after the interaction is switched off at the moment $t = \tau$. We are interested in how energy can be transferred to QB more efficiently. For this purpose, we study the performance of the QB at the end of the charging process.

For convenience, we assume that the initial state of the total system is

$$|\psi(0)\rangle = |1_C\rangle|0_B\rangle(\alpha|10\rangle + \beta|01\rangle), \quad (7)$$

where $|1_C\rangle$ and $|0_B\rangle$ signify that the charger and QB are in the excited state and ground state, respectively, whereas $\alpha|10\rangle + \beta|01\rangle$ indicates that the cavities are in an entangled-like state. The initial entanglement can be characterized by the concurrence C , as defined in Refs. [54–58]. For the entangled states $\alpha|10\rangle + \beta|01\rangle$ we consider, the concurrence can be immediately calculated as $C = 2|\alpha\beta|$ [54]. In the following, we aim to determine the conditions for achieving optimal charging performance of the QB when the entangled coupled cavity is used as the working medium for QB charging. It is worth noting that, in our discussion, we will treat the composite system as a closed quantum system, neglecting the dissipative effects associated with relaxation and dephasing phenomena. This is possible when the typical relaxation time t_r and dephasing time t_ϕ are significantly longer than the evolution time τ under consideration, i.e., $t_r, t_\phi \gg \tau$ [59,60].

Starting from the initial state [i.e., Eq. (7)], the total evolved pure state reads

$$\begin{aligned}
 |\psi(t)\rangle = & c_1(t)|1_C\rangle|0_B\rangle|01\rangle + c_2(t)|1_C\rangle|0_B\rangle|10\rangle \\
 & + c_3(t)|0_C\rangle|1_B\rangle|01\rangle + c_4(t)|0_C\rangle|1_B\rangle|10\rangle \\
 & + c_5(t)|0_C\rangle|0_B\rangle|11\rangle + c_6(t)|0_C\rangle|0_B\rangle|20\rangle \\
 & + c_7(t)|0_C\rangle|0_B\rangle|02\rangle + c_8(t)|1_C\rangle|1_B\rangle|00\rangle. \quad (8)
 \end{aligned}$$

From the Schrödinger equation, the time evolution of the total system in the interaction picture is determined by the set of differential equations in Appendix A. By solving the differential equations, these probability amplitudes [i.e., $c_1(t) \dots c_8(t)$] can be obtained. The reduced density matrix of the QB can be obtained by tracing over the freedoms of the cavity field and the charger. Then according to Eqs. (1) to (3), the stored energy $E_B(\tau)$, the average charging power $P_B(\tau)$, and the ergotropy $W_B(\tau)$ are represented by

$$\begin{aligned}
 E_B(\tau) &= \omega(|c_3(\tau)|^2 + |c_4(\tau)|^2 + |c_8(\tau)|^2), \\
 P_B(\tau) &= \omega(|c_3(\tau)|^2 + |c_4(\tau)|^2 + |c_8(\tau)|^2)/\tau, \\
 W_B(\tau) &= \omega[2(|c_3(\tau)|^2 + |c_4(\tau)|^2 + |c_8(\tau)|^2) - 1] \\
 &\quad \Theta\left[(|c_3(\tau)|^2 + |c_4(\tau)|^2 + |c_8(\tau)|^2) - \frac{1}{2} \right], \quad (9)
 \end{aligned}$$

where $\Theta(x - x_0)$ is the Heaviside function. Then, according to Eq. (9), the effect of the presence of entangled coupled-cavity on the charging performance of the QB can be analyzed.

First, we show how the cavity m_1 - m_2 initial entanglement C affects $E_B(\tau)$, $P_B(\tau)$, and $W_B(\tau)$ in Figs. 2(a) to 2(c). We find that higher entanglement C results in better charging performance of the QB [i.e., the larger $E_B(\tau)$, $P_B(\tau)$, and $W_B(\tau)$]. To fully understand the influence of entanglement on the charging process and achieve the optimal QB, we also plot the variations of E_{\max} , P_{\max} , and W_{\max} with the entanglement C and the coupling strength Ω/ω between the two cavities, as shown in Figs. 2(d) to 2(f). It is clear that E_{\max} , P_{\max} , and W_{\max} will be at their optimal values when the cavities are initially in the maximally entangled ($C = 1$) and there is no coupling $\Omega/\omega = 0$ between the cavities. In particular, when $C = 1$ and $\Omega/\omega = 0$, the stored energy of the QB reaches its maximum value and the energy can be fully extracted. Therefore, to obtain the optimal performance of the QB when the two entangled coupled cavities mediate the charging process, the cavities should be set initially to be in the maximally entangled state with no coupling between them.

Now, one may wonder why the cavity m_1 - m_2 initial entanglement and the coupling between the cavities cause the above effects on the performance of the QB. To account for the effect of the coupling, we apply the Bogoliubov transformations to the Hamiltonian of the total system [i.e., Eq. (4)]. See Appendix B for details of the procedure. We find that the presence of the coupling leads to a frequency detuning between the cavities and the QB or charger. This means a non-maximum effective coupling between the QB or charger and the cavities can occur, which is not conducive to the energy flow of the charger to the QB and then leads to the existence of coupling will be detrimental to the charging process of a QB. According to Ref. [48], the QB-charger entanglement can lead to more energy injection into the QB and consequently more ergotropy. Then to illustrate the effect of the cavity m_1 - m_2

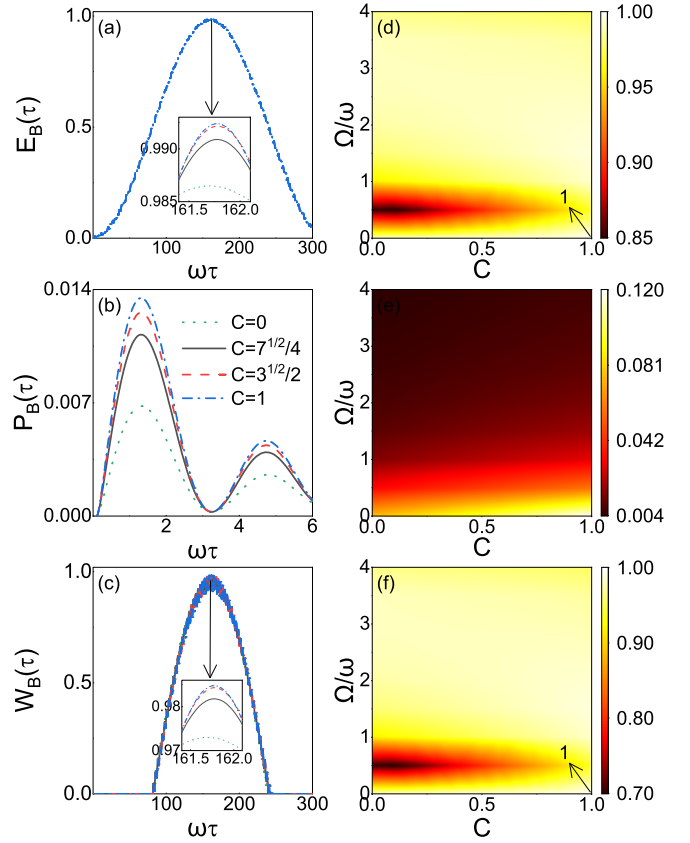


FIG. 2. Behaviors of (a) stored energy $E_B(\tau)$ (in units of ω), (b) average charging power $P_B(\tau)$ (in units of ω), and (c) ergotropy $W_B(\tau)$ (in units of ω) as a function of $\omega\tau$ for the different initial cavity $m_1 - m_2$ entanglement C . Behaviors of (d) maximum stored energy E_{\max} (in units of ω), (e) maximum average charging power P_{\max} (in units of ω), and (f) maximum ergotropy W_{\max} (in units of ω) as a function of C and the coupling strength Ω/ω between the cavity m_1 and the cavity m_2 . The parameters are (a)–(c) $\kappa = 0.1\omega$ and $\Omega = 2\omega$; (d)–(f) $\kappa = 0.1\omega$.

initial entanglement C on the performance of the QB, we start from the QB-charger entanglement S . See Appendix C for details. In Fig. 3, we show the dynamics behavior of S as a function of $\omega\tau$ for the different values of C . We find that as C increases, the value of S also increases. This suggests that an increase in the m_1 - m_2 initial entanglement leads to an increase in the QB-charger entanglement, which in turn allows more energy to be injected into the QB. That is to say, the greater QB-charger entanglement is the reason for the improved battery performance.

IV. MULTIPLE COUPLED-CAVITY MEDIATED THE CHARGING PROCESS OF A QB

To obtain the optimal QB, we also study the case of multicavity mediating the QB charging process. Since the measurement of many-body entanglement is currently difficult and is not the focus of our paper, we mainly concentrate on the effect of the coupling between the nearest-neighbor cavities on the charging performance of the QB.

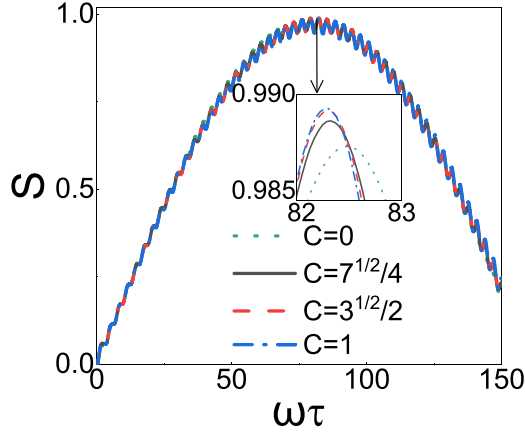


FIG. 3. Dynamics behavior of the QB-charger entanglement S as a function of $\omega\tau$ for the different cavity $m_1 - m_2$ initial entanglement C . The parameters are $\kappa = 0.1\omega$ and $\Omega = 2\omega$.

To gain a comprehensive understanding of how the coupling affects the performance of the QB, we consider scenarios where the multiple coupled-cavity is initially in both entangled and unentangled states. The total system Hamiltonian is given by $H = H_0 + f(t)H_I$. The free Hamiltonian H_0 is written as

$$H_0 = \frac{\omega}{2}\sigma_z^B + \frac{\omega}{2}\sigma_z^C + \sum_{n=1}^N \omega a_n^\dagger a_n. \quad (10)$$

Each term from left to right in Eq. (10) represents the free Hamiltonian for the QB, charger, and cavities, respectively. Then the interaction Hamiltonian H_I is denoted as

$$H_I = \sum_{n=1}^N \kappa(\sigma_+^B a_n + \sigma_-^B a_n^\dagger) + \sum_{n=1}^N \kappa(\sigma_+^C a_n + \sigma_-^C a_n^\dagger) + \sum_{\langle ij \rangle} \Omega(a_i^\dagger a_j + a_i a_j^\dagger), \quad (11)$$

where the first term represents the interaction between the QB and the cavities, the second term represents the interaction between the charger and the cavities, and the third term refers to the interaction between the nearest-neighbor cavities. $\langle ij \rangle$ means the nearest-neighbor cavities.

A. Multiple entangled coupled-cavity mediated the charging process of a QB

We first discuss the impact of the coupling between the nearest cavities on the QB's performance in the entangled coupled-cavity array scenario, as shown in Fig. 4. For convenience, we consider four coupled cavities. We assume the initial state of the total system to be

$$|\psi(0)\rangle = |1_C\rangle|0_B\rangle(\alpha_1|1000\rangle + \alpha_2|0100\rangle + \alpha_3|0010\rangle + \alpha_4|0001\rangle). \quad (12)$$

The charger is initially in the excited state $|1_C\rangle$, the QB is initially in the ground state $|0_B\rangle$, and the four cavities are in the entangled state $\alpha_1|1000\rangle + \alpha_2|0100\rangle + \alpha_3|0010\rangle + \alpha_4|0001\rangle$. For the sake of convenience, we consider $\alpha_1 = \alpha_2 = \alpha_3 = \alpha_4 = 1/2$. Since the total system is in the dual excitation

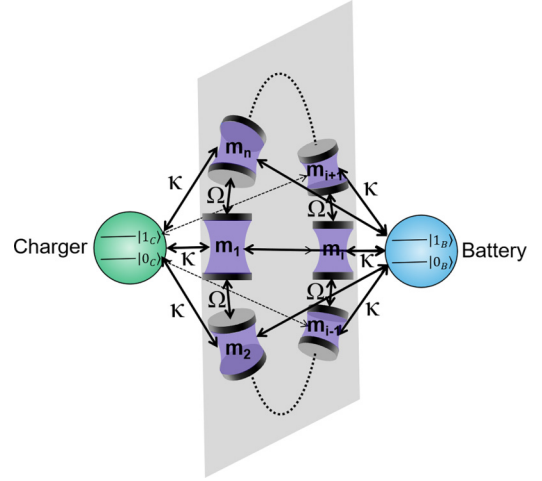


FIG. 4. Schematic representation of the multiple coupled-cavity that mediate energy transfer between the QB and the charger.

space, the evolution state of the system at any time t can be written as

$$\begin{aligned} |\psi(t)\rangle = & c_1|1_C\rangle|0_B\rangle|1000\rangle + c_2|1_C\rangle|0_B\rangle|0100\rangle \\ & + c_3|1_C\rangle|0_B\rangle|0010\rangle + c_4|1_C\rangle|0_B\rangle|0001\rangle \\ & + c_5|0_C\rangle|1_B\rangle|1000\rangle + c_6|0_C\rangle|1_B\rangle|0100\rangle \\ & + c_7|0_C\rangle|1_B\rangle|0010\rangle + c_8|0_C\rangle|1_B\rangle|0001\rangle \\ & + c_9|0_C\rangle|0_B\rangle|1100\rangle + c_{10}|0_C\rangle|0_B\rangle|1010\rangle \\ & + c_{11}|0_C\rangle|0_B\rangle|1001\rangle + c_{12}|0_C\rangle|0_B\rangle|0110\rangle \\ & + c_{13}|0_C\rangle|0_B\rangle|0101\rangle + c_{14}|0_C\rangle|0_B\rangle|0011\rangle \\ & + c_{15}|0_C\rangle|0_B\rangle|2000\rangle + c_{16}|0_C\rangle|0_B\rangle|0200\rangle \\ & + c_{17}|0_C\rangle|0_B\rangle|0020\rangle + c_{18}|0_C\rangle|0_B\rangle|0002\rangle \\ & + c_{19}|1_C\rangle|1_B\rangle|0000\rangle. \end{aligned} \quad (13)$$

According to the Schrödinger equation, the time-dependent amplitudes (i.e., c_1, c_2, \dots, c_{19}) are determined by the system of differential equations provided in Appendix D. By numerically solving these differential equations, these probability amplitudes can be obtained. Then the reduced density matrix of the QB can be obtained by tracing over the degrees of freedom of the charger and the four cavities. Based on Eqs. (1) to (3), the stored energy $E_B(\tau)$, the average charging power $P_B(\tau)$, and the ergotropy $W_B(\tau)$ can be expressed as

$$\begin{aligned} E_B(\tau) &= \omega(|c_5|^2 + |c_6|^2 + |c_7|^2 + |c_8|^2 + |c_{19}|^2), \\ P_B(\tau) &= \omega(|c_5|^2 + |c_6|^2 + |c_7|^2 + |c_8|^2 + |c_{19}|^2)/\tau, \\ W_B(\tau) &= \omega[2(|c_5|^2 + |c_6|^2 + |c_7|^2 + |c_8|^2 \\ & + |c_{19}|^2) - 1]\Theta[(|c_5|^2 + |c_6|^2 + |c_7|^2 \\ & + |c_8|^2 + |c_{19}|^2) - \frac{1}{2}]. \end{aligned} \quad (14)$$

The influence of the coupling between the nearest-neighbor cavities on the performance of the QB can be analyzed from Eq. (14).

In Fig. 5, we plot the variations of maximum stored energy E_{\max} , maximum average charging power P_{\max} , and

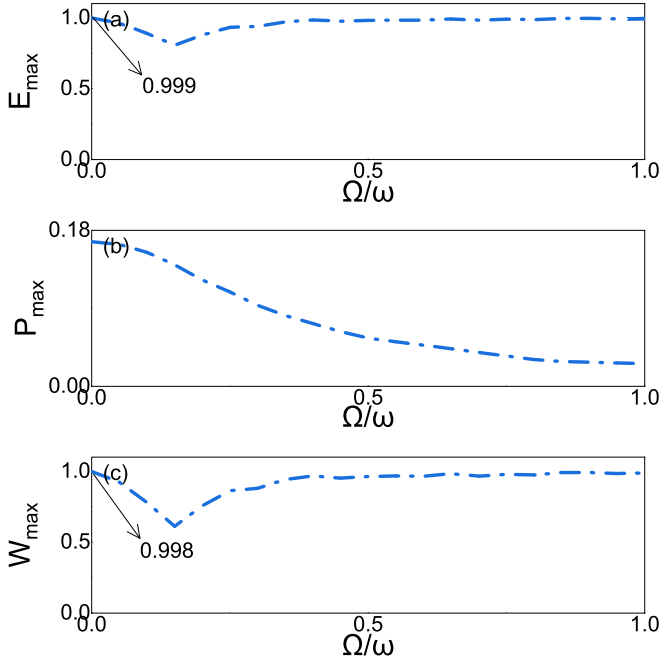


FIG. 5. In the scenario of multiple entangled coupled-cavity, behaviors of (a) maximum stored energy E_{\max} (in units of ω), (b) maximum average charging power P_{\max} (in units of ω), and (c) maximum ergotropy W_{\max} (in units of ω) as a function of Ω/ω between the nearest-neighbor cavities. The parameter is $\kappa = 0.1\omega$.

maximum ergotropy W_{\max} with respect to Ω/ω between the nearest-neighbor cavities. Similar to Fig. 2, reducing of the coupling Ω/ω can improve the maximum value of E_{\max} , P_{\max} , and W_{\max} . Furthermore, we find that, compared to using two entangled coupled-cavity, by employing four of the entangled-coupled cavities further would enhance the average charging power of the QB. This enhancement can be attributed to the increased number of cavities, which strengthens the effective coupling between the QB and the cavities, as well as between the charger and the cavities. To achieve the optimal charging performance of the QB, an array of large-scale entangled uncoupled cavities is required.

B. Multiple unentangled coupled-cavity mediated the charging process of a QB

In the previous section, we investigate the effect of inter-cavity coupling on the charging performance of the QB in the multiple entangled coupled-cavity scenario. To fully understand the influence of the coupling between the nearest-neighbor cavities on the charging performance of the QB, the initial multiple unentangled coupled cavity should also be considered with equal importance. We assume that the initial state of the total system can be written as

$$|\psi(0)\rangle = |1_C\rangle|1000\rangle|0_B\rangle. \quad (15)$$

Equation (15) can be obtained by Eq. (12) (that is, setting $\alpha_1 = 1$ and $\alpha_2 = \alpha_3 = \alpha_4 = 0$). The evolution state of the total system at any time can be written as Eq. (13). Then according to the same process and steps as in the previous section, the stored energy $E_B(\tau)$, average power $P_B(\tau)$, and

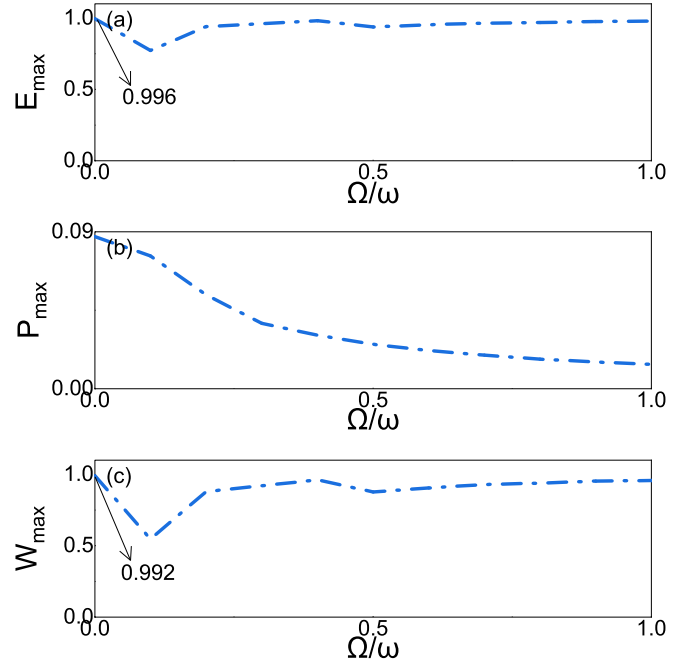


FIG. 6. In the scenario of multiple unentangled coupled-cavity, behaviors of (a) maximum stored energy E_{\max} (in units of ω), (b) maximum average charging power P_{\max} (in units of ω), and (c) maximum ergotropy W_{\max} (in units of ω) as a function of Ω/ω between the nearest-neighbor cavities. The parameter is $\kappa = 0.1\omega$.

ergotropy $W_B(\tau)$ of the QB can be expressed as Eq. (14). In the multiple unentangled coupled-cavity scenario, the effect of the coupling Ω/ω between the nearest-neighbor cavities on the performance of the QB can be described.

The variation of E_{\max} , P_{\max} , and W_{\max} with Ω/ω has been shown in Fig. 6. The smaller Ω/ω can excite the larger E_{\max} , P_{\max} , and W_{\max} . However, it is noted that, compared with Fig. 5, the scenario of multiple entangled coupled-cavity is more beneficial to the QB charging process under the same conditions. Therefore, the entangled uncoupled-cavity array is required to realize the optimal QB.

C. Effect of the scale of the coupled-cavity on the performance of a QB

In the previous two sections, we focus on the effect of the coupling between the nearest-neighbor cavities on the performance of the QB when the initial states of multiple coupled-cavity are different. The scale effect of the coupled-cavity is not considered. Currently, large-scale coupled-cavity array can be realized by superconducting circuits [61]. Coupled-cavity arrays play an important role in large-scale quantum information processing and quantum network construction. Therefore, the effect of the scale of the coupled-cavity array on the charging performance of the QB should be carefully considered.

To facilitate the study of the effect of the size of the coupled cavity on the performance of the QB, the whole system is considered in the single excitation space. We assume that the initial state of the entire system is

$$|\psi(0)\rangle = |1_C\rangle|0 \dots 0\rangle|0_B\rangle. \quad (16)$$

Here the charger is in the excited state $|1_C\rangle$, the QB and the cavity array are in their ground states (i.e., $|0_B\rangle$ and $|0 \cdots 0\rangle$), respectively. The evolution state of the total system at any time t can be written as

$$|\psi(t)\rangle = g_1(t)|1_C\rangle|0_B\rangle|0 \cdots 0\rangle + g_2(t)|0_C\rangle|1_B\rangle|0 \cdots 0\rangle + \sum_{n=1}^N c_n(t)|0_C\rangle|0_B\rangle|0 \cdots 1 \cdots 0\rangle, \quad (17)$$

where $|0 \cdots 0\rangle$ represents the cavity array in the ground state, and $|0 \cdots 1 \cdots 0\rangle$ represents the n th cavity in the excited state while the other cavities are in the ground state. According to the Schrödinger equation, the time evolution of the total system in the interaction picture can be determined by the following differential equations:

$$\begin{aligned} \dot{g}_1(t) &= -i \sum_{n=1}^N \kappa c_n(t), \\ \dot{g}_2(t) &= -i \sum_{n=1}^N \kappa c_n(t), \\ \sum_{n=1}^N \dot{c}_n(t) &= -iN\kappa g_1(t) - iN\kappa g_2(t) - i \sum_{n=1}^N 2\Omega c_n(t). \end{aligned} \quad (18)$$

The above differential equations can be solved by means of standard Laplace transformations combined with numerical simulations to obtain the reduced density operators of the QB. According to Eqs. (1) to (3), the stored energy $E_B(\tau)$, average charging power $P_B(\tau)$, and ergotropy $W_B(\tau)$ are represented by

$$\begin{aligned} E_B(\tau) &= \omega |g_2(\tau)|^2, \\ P_B(\tau) &= \omega |g_2(\tau)|^2 / \tau, \\ W_B(\tau) &= \omega [2|g_2(\tau)|^2 - 1] \Theta[|g_2(\tau)|^2 - \frac{1}{2}]. \end{aligned} \quad (19)$$

In the following, the effect of the number N of cavities in the array and the coupling Ω/ω on the QB's performance can be investigated.

Figures 7(a) to 7(c) depict the influence of the number N of cavities on the parameters $E_B(\tau)$, $P_B(\tau)$, and $W_B(\tau)$. The parameter N exerts a negligible influence on the maxima of $E_B(\tau)$ and $W_B(\tau)$, contrasting with its effect on $P_B(\tau)$. An escalation in N is observed to markedly augment the charging power of the QB, suggesting that a rapid charging regimen is contingent upon an increased number of cavities. Then to elucidate the optimal battery performance, the impact of N and Ω/ω on E_{\max} , P_{\max} , and W_{\max} is delineated within Figs. 7(d) to 7(f). It becomes apparent that the achievement of superior battery performance is predicated upon a large N and minimal intercavity coupling. Specifically, at $N = 6$ with zero coupling, the QB reaches full charge capacity, and the energy is entirely extractable, which is exactly what is needed to realize the performance of an ideal QB. Consequently, the utilization of a cavity array as the medium for battery charging mandates an increased number of cavities in conjunction with an absence of coupling between them to secure optimal battery charging performance.

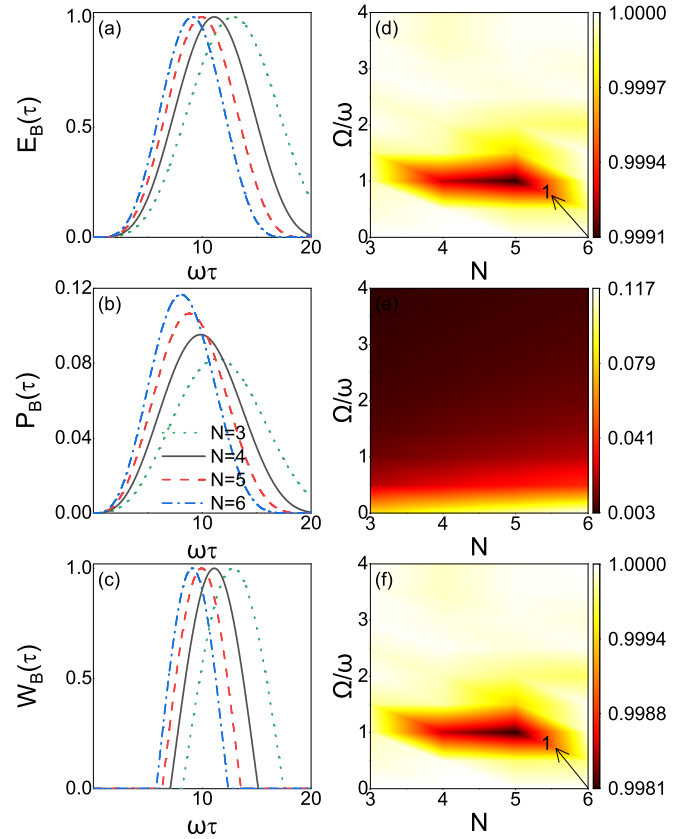


FIG. 7. Behaviors of (a) stored energy $E_B(\tau)$ (in units of ω), (b) average charging power $P_B(\tau)$ (in units of ω), and (c) ergotropy $W_B(\tau)$ (in units of ω) as a function of $\omega\tau$ for the different numbers N of cavities. Behaviors of (d) maximum stored energy E_{\max} (in units of ω), (e) maximum average charging power P_{\max} (in units of ω), and (f) maximum ergotropy W_{\max} (in units of ω) as a function of N and the coupling strength Ω/ω between the nearest-neighbor cavities. The parameters are (a)–(c) $\kappa = 0.1\omega$ and $\Omega/\omega = 0$; (d)–(f) $\kappa = 0.1\omega$.

V. CONCLUSION

We investigated the charging performance of a QB with an entangled coupled-cavity array as the working medium. It was demonstrated that the charging performance is optimal in the two-cavity case when cavities were initially in a maximum entangled state without cavity couplings. We elucidated the impact of initial cavity-cavity entanglement and intercavity coupling on the charging performance of the QB by examining the QB-charger entanglement and the frequency detuning between the QB and charger and the cavities. Subsequently, we extended our model to the scenario involving the multicavity. Similar to the two-cavity case, the ideal performance of the QB was obtained without inter-cavity coupling, which was independent of whether the cavities were initially in the entangled or separated state. Furthermore, it was found that the average charging power of the QB under the entangled coupled-cavity array can be further improved by increasing the number of cavities. These results can provide some theoretical guidance for realizing the optimal charging process of a QB with the working medium of an entangled coupled-cavity array.

Finally, we discuss the experimental implementations of our model. A promising platform in the realm of quantum technology is the superconducting circuits [62], which is renowned for its excellent controllability and its compatibility with various interfaces. Specifically, the coupled-cavity array can be made of superconducting microwave cavities embedded with superconducting quantum interference device (SQUID) loops [63,64], and the coupling strength between the nearest-neighbor cavities can be modulated by manipulating the capacitance. Based on the feasibility of this experiment, we believe that our research will have a positive impact on the realization of the optimal charging performance of quantum batteries in the future.

ACKNOWLEDGMENTS

This work was supported by the National Natural Science Foundation of China (Grant No. 12204348), and Natural Science Foundation of Tianjin city (Grants No. 23JCYBJC00150 and No. 16JCQJNC01600).

APPENDIX A: DIFFERENTIAL EQUATIONS FOR THE PROBABILITY AMPLITUDE OF THE EVOLUTION STATE OF THE TOTAL SYSTEM WHEN TWO ENTANGLED COUPLED-CAVITY MEDIATED THE CHARGING PROCESS OF A QB

Based on the Schrödinger equation and Eqs. (5) to (8), we can obtain a series of differential equations that the probability amplitudes satisfy

$$\begin{aligned}
 \dot{c}_1(t) &= -ikc_5(t) + (-i)\sqrt{2}\kappa c_7(t) + (-i)\kappa c_8(t) \\
 &\quad + (-i)\Omega c_2(t), \\
 \dot{c}_2(t) &= -ikc_5(t) + (-i)\sqrt{2}\kappa c_6(t) + (-i)\kappa c_8(t) \\
 &\quad + (-i)\Omega c_1(t), \\
 \dot{c}_3(t) &= -ikc_8(t) + (-i)\kappa c_5(t) + (-i)\sqrt{2}\kappa c_7(t) \\
 &\quad + (-i)\Omega c_4(t), \\
 \dot{c}_4(t) &= -ikc_8(t) + (-i)\kappa c_5(t) + (-i)\sqrt{2}\kappa c_6(t) \\
 &\quad + (-i)\Omega c_3(t), \\
 \dot{c}_5(t) &= -ikc_1(t) + (-i)\kappa c_2(t) + (-i)\kappa c_3(t) \\
 &\quad + (-i)\kappa c_4(t) + (-i)\sqrt{2}\Omega c_7(t) + (-i)\sqrt{2}\Omega c_6(t), \\
 \dot{c}_6(t) &= -i\sqrt{2}\kappa c_2(t) + (-i)\sqrt{2}\kappa c_4(t) + (-i)\sqrt{2}\Omega c_5(t), \\
 \dot{c}_7(t) &= -i\sqrt{2}\kappa c_1(t) + (-i)\sqrt{2}\kappa c_3(t) + (-i)\sqrt{2}\Omega c_5(t), \\
 \dot{c}_8(t) &= -ikc_1(t) + (-i)\kappa c_2(t) + (-i)\kappa c_3(t) \\
 &\quad + (-i)\kappa c_4(t). \tag{A1}
 \end{aligned}$$

APPENDIX B: BOSE BOGOLIUBOV TRANSFORMATIONS

To elucidate the impact of the coupling strength Ω/ω between the cavity fields on the performance of the QB, we perform a Bogoliubov transformation in Eqs. (5) and (6)

$$a_1 = ud_1 + vd_2, \quad a_2 = vd_1 + ud_2. \tag{B1}$$

To be a unitary transformation, the coefficients u and v must satisfy the relation

$$u^2 + v^2 = 1. \tag{B2}$$

Taking Eq. (B1) into Eqs. (5) and (6), and setting the coupling term between d_1 and d_2 to zero, can be obtained

$$uv^* + u^*v = -\Omega/\omega, \tag{B3}$$

where v^* and u^* denote the complex conjugate of v and u , respectively. Then the Hamiltonian of the total system [i.e., Eq. (4)] can be written as

$$\begin{aligned}
 H &= \omega\sigma_z^B/2 + \omega\sigma_z^C/2 + (\omega - \Omega^2/\omega)d_1^\dagger d_1 \\
 &\quad + (\omega - \Omega^2/\omega)d_2^\dagger d_2 + \kappa(M\sigma_+^B d_1 + M^*\sigma_-^B d_1^\dagger + M\sigma_+^C d_2 \\
 &\quad + M^*\sigma_-^C d_2^\dagger + \kappa(M\sigma_+^C d_1 + M^*\sigma_-^C d_1^\dagger + M\sigma_+^C d_2 \\
 &\quad + M^*\sigma_-^C d_2^\dagger), \tag{B4}
 \end{aligned}$$

where $M = u + v$.

APPENDIX C: QB-CHARGER ENTANGLEMENT

According to Eq. (8), the evolution density matrix of the total system can be obtained $\rho(t) = |\psi(t)\rangle\langle\psi(t)|$. By tracing out the freedom of the cavities, the reduced density matrices of the QB-charger under the basis $\{|11\rangle, |10\rangle, |01\rangle, |00\rangle\}$ can be obtained, i.e.,

$$\rho_{CB}(t) = \begin{pmatrix} |c_8|^2 & 0 & 0 & 0 \\ 0 & |c_1|^2 + |c_2|^2 & c_2 c_4^* + c_1 c_3^* & 0 \\ 0 & c_2^* c_4 + c_1^* c_3 & |c_3|^2 + |c_4|^2 & 0 \\ 0 & 0 & 0 & m \end{pmatrix}, \tag{C1}$$

where $m = |c_5|^2 + |c_6|^2 + |c_7|^2$. For the biqubit system, the genuinely multiqubit (GM) concurrence can be simplified to the Wootters's concurrence. For the two-qubit state $\rho_{CB}(t)$, the GM concurrence can be immediately obtained $S = 2 \max\{0, |c_2^* c_4 + c_1^* c_3| - \sqrt{|c_8|^2(|c_5|^2 + |c_6|^2 + |c_7|^2)}\}$.

APPENDIX D: DIFFERENTIAL EQUATIONS FOR THE PROBABILITY AMPLITUDE OF THE EVOLUTION STATE OF THE TOTAL SYSTEM WHEN MULTIPLE COUPLED-CAVITY MEDIATED THE CHARGING PROCESS OF A QB

According to the Schrödinger equation and Eqs. (10) to (13), the differential equation for the probability amplitude of the evolution state of the total system can be written as

$$\begin{aligned}
 \dot{c}_1 &= -ikc_9 + (-i)\kappa c_{10} + (-i)\kappa c_{11} + (-i)\kappa c_{19} \\
 &\quad + (-i)\sqrt{2}\kappa c_{15} + (-i)\Omega c_2 + (-i)\Omega c_4, \\
 \dot{c}_2 &= -ikc_9 + (-i)\kappa c_{12} + (-i)\kappa c_{13} + (-i)\kappa c_{19} \\
 &\quad + (-i)\sqrt{2}\kappa c_{16} + (-i)\Omega c_1 + (-i)\Omega c_3, \\
 \dot{c}_3 &= -ikc_{10} + (-i)\kappa c_{12} + (-i)\kappa c_{14} + (-i)\kappa c_{19} \\
 &\quad + (-i)\sqrt{2}\kappa c_{17} + (-i)\Omega c_2 + (-i)\Omega c_4,
 \end{aligned}$$

$$\begin{aligned}
\dot{c}_4 &= -ikc_{11} + (-i)\kappa c_{13} + (-i)\kappa c_{14} + (-i)\kappa c_{19} \\
&\quad + (-i)\sqrt{2}\kappa c_{18} + (-i)\Omega c_1 + (-i)\Omega c_3, \\
\dot{c}_5 &= -ikc_9 + (-i)\kappa c_{10} + (-i)\kappa c_{11} + (-i)\kappa c_{19} \\
&\quad + (-i)\sqrt{2}\kappa c_{15} + (-i)\Omega c_6 + (-i)\Omega c_8, \\
\dot{c}_6 &= -ikc_9 + (-i)\kappa c_{12} + (-i)\kappa c_{13} + (-i)\kappa c_{19} \\
&\quad + (-i)\sqrt{2}\kappa c_{16} + (-i)\Omega c_7 + (-i)\Omega c_5, \\
\dot{c}_7 &= -ikc_{10} + (-i)\kappa c_{12} + (-i)\kappa c_{14} + (-i)\kappa c_{19} \\
&\quad + (-i)\sqrt{2}\kappa c_{17} + (-i)\Omega c_6 + (-i)\Omega c_8, \\
\dot{c}_8 &= -ikc_{11} + (-i)\kappa c_{13} + (-i)\kappa c_{14} + (-i)\kappa c_{19} \\
&\quad + (-i)\sqrt{2}\kappa c_{18} + (-i)\Omega c_5 + (-i)\Omega c_7, \\
\dot{c}_9 &= -ikc_1 + (-i)\kappa c_2 + (-i)\kappa c_5 + (-i)\kappa c_6 \\
&\quad + (-i)\sqrt{2}\Omega c_{15} + (-i)\sqrt{2}\Omega c_{16} + (-i)\Omega c_{10} \\
&\quad + (-i)\Omega c_{13}, \\
\dot{c}_{10} &= -ikc_1 + (-i)\kappa c_3 + (-i)\kappa c_5 + (-i)\kappa c_7 \\
&\quad + (-i)\Omega c_9 + (-i)\Omega c_{11} + (-i)\Omega c_{12} + (-i)\Omega c_{14}, \\
\dot{c}_{11} &= -ikc_1 + (-i)\kappa c_4 + (-i)\kappa c_5 + (-i)\kappa c_8 \\
&\quad + (-i)\sqrt{2}\Omega c_{15} + (-i)\sqrt{2}\Omega c_{18} + (-i)\Omega c_{10} \\
&\quad + (-i)\Omega c_{13}, \\
\dot{c}_{12} &= -ikc_2 + (-i)\kappa c_3 + (-i)\kappa c_6 + (-i)\kappa c_7 \\
&\quad + (-i)\sqrt{2}\Omega c_{16} + (-i)\sqrt{2}\Omega c_{17} + (-i)\Omega c_{10} \\
&\quad + (-i)\Omega c_{13}, \\
\dot{c}_{13} &= -ikc_2 + (-i)\kappa c_4 + (-i)\kappa c_6 + (-i)\kappa c_8 \\
&\quad + (-i)\Omega c_9 + (-i)\Omega c_{11} + (-i)\Omega c_{12} + (-i)\Omega c_{14}, \\
\dot{c}_{14} &= -ikc_3 + (-i)\kappa c_4 + (-i)\kappa c_7 + (-i)\kappa c_8 \\
&\quad + (-i)\sqrt{2}\Omega c_{17} + (-i)\sqrt{2}\Omega c_{18} + (-i)\Omega c_{10} \\
&\quad + (-i)\Omega c_{17}, \\
\dot{c}_{15} &= -i\sqrt{2}\kappa c_1 + (-i)\sqrt{2}\kappa c_5 + (-i)\sqrt{2}\Omega c_9 \\
&\quad + (-i)\sqrt{2}\Omega c_{11}, \\
\dot{c}_{16} &= -i\sqrt{2}\kappa c_2 + (-i)\sqrt{2}\kappa c_6 + (-i)\sqrt{2}\Omega c_9 \\
&\quad + (-i)\sqrt{2}\Omega c_{12}, \\
\dot{c}_{17} &= -i\sqrt{2}\kappa c_3 + (-i)\sqrt{2}\kappa c_7 + (-i)\sqrt{2}\Omega c_{12} \\
&\quad + (-i)\sqrt{2}\Omega c_{14}, \\
\dot{c}_{18} &= -i\sqrt{2}\kappa c_4 + (-i)\sqrt{2}\kappa c_8 + (-i)\sqrt{2}\Omega c_{11} \\
&\quad + (-i)\sqrt{2}\Omega c_{14}, \\
\dot{c}_{19} &= -ikc_1 + (-i)\kappa c_2 + (-i)\kappa c_3 + (-i)\kappa c_4 \\
&\quad + (-i)\kappa c_5 + (-i)\kappa c_6 + (-i)\kappa c_7 + (-i)\kappa c_8. \quad (\text{D1})
\end{aligned}$$

-
- [1] F. Caravelli, G. Coulter-De Wit, L. P. García-Pintos, and A. Hamma, *Phys. Rev. Res.* **2**, 023095 (2020).
- [2] S. Julià-Farré, T. Salamon, A. Riera, M. N. Bera, and M. Lewenstein, *Phys. Rev. Res.* **2**, 023113 (2020).
- [3] A. C. Santos, B. Çakmak, S. Campbell, and N. T. Zinner, *Phys. Rev. E* **100**, 032107 (2019).
- [4] F. Barra, *Phys. Rev. Lett.* **122**, 210601 (2019).
- [5] G. M. Andolina, D. Farina, A. Mari, V. Pellegrini, V. Giovannetti, and M. Polini, *Phys. Rev. B* **98**, 205423 (2018).
- [6] A. C. Santos, A. Saguia, and M. S. Sarandy, *Phys. Rev. E* **101**, 062114 (2020).
- [7] F. H. Kamin, F. T. Tabesh, S. Salimi, and A. C. Santos, *Phys. Rev. E* **102**, 052109 (2020).
- [8] R. Alicki and M. Fannes, *Phys. Rev. E* **87**, 042123 (2013).
- [9] K. Xu, H. G. Li, Z. G. Li, H. J. Zhu, G. F. Zhang, and W. M. Liu, *Phys. Rev. A* **106**, 012425 (2022).
- [10] K. Xu, H.-J. Zhu, G.-F. Zhang, and W.-M. Liu, *Phys. Rev. E* **104**, 064143 (2021).
- [11] F. C. Binder, S. Vinjanampathy, K. Modi, and J. Goold, *New J. Phys.* **17**, 075015 (2015).
- [12] F. Campaioli, F. A. Pollock, F. C. Binder, L. Céleri, J. Goold, S. Vinjanampathy, and K. Modi, *Phys. Rev. Lett.* **118**, 150601 (2017).
- [13] N. Friis and M. Huber, *Quantum* **2**, 61 (2018).
- [14] J. Q. Quach and W. J. Munro, *Phys. Rev. Appl.* **14**, 024092 (2020).
- [15] F. Pirmoradian and K. Mølmer, *Phys. Rev. A* **100**, 043833 (2019).
- [16] Y. Huangfu and J. Jing, *Phys. Rev. E* **104**, 024129 (2021).
- [17] W. Lu, J. Chen, L.-M. Kuang, and X. Wang, *Phys. Rev. A* **104**, 043706 (2021).
- [18] W.-L. Song, H.-B. Liu, B. Zhou, W.-L. Yang, and J.-H. An, *Phys. Rev. Lett.* **132**, 090401 (2024).
- [19] F.-Q. Dou, H. Zhou, and J.-A. Sun, *Phys. Rev. A* **106**, 032212 (2022).
- [20] W.-X. Guo, F.-M. Yang, and F.-Q. Dou, *Phys. Rev. A* **109**, 032201 (2024).
- [21] G. M. Andolina, M. Keck, A. Mari, M. Campisi, V. Giovannetti, and M. Polini, *Phys. Rev. Lett.* **122**, 047702 (2019).
- [22] A. Crescente, M. Carrega, M. Sassetti, and D. Ferraro, *Phys. Rev. B* **102**, 245407 (2020).
- [23] L. Peng, W. B. He, S. Chesi, H. Q. Lin, and X. W. Guan, *Phys. Rev. A* **103**, 052220 (2021).
- [24] T. P. Le, J. Levinsen, K. Modi, M. M. Parish, and F. A. Pollock, *Phys. Rev. A* **97**, 022106 (2018).
- [25] S. Ghosh, T. Chanda, and A. Sen(De), *Phys. Rev. A* **101**, 032115 (2020).

- [26] A. Brataas, Y. Tserkovnyak, G. E. W. Bauer, and B. I. Halperin, *Phys. Rev. B* **66**, 060404(R) (2002).
- [27] D. Rossini, G. M. Andolina, D. Rosa, M. Carrega, and M. Polini, *Phys. Rev. Lett.* **125**, 236402 (2020).
- [28] J. Carrasco, J. R. Maze, C. Hermann-Avigliano, and F. Barra, *Phys. Rev. E* **105**, 064119 (2022).
- [29] Y. Y. Zhang, T. R. Yang, L. Fu, and X. Wang, *Phys. Rev. E* **99**, 052106 (2019).
- [30] G. M. Andolina, M. Keck, A. Mari, V. Giovannetti, and M. Polini, *Phys. Rev. B* **99**, 205437 (2019).
- [31] L. Wang, S.-Q. Liu, F.-L. Wu, H. Fan, and S.-Y. Liu, *Phys. Rev. A* **108**, 062402 (2023).
- [32] A. Crescente, D. Ferraro, M. Carrega, and M. Sassetti, *Phys. Rev. Res.* **4**, 033216 (2022).
- [33] L. P. García-Pintos, A. Hamma, and A. del Campo, *Phys. Rev. Lett.* **125**, 040601 (2020).
- [34] D. Rossini, G. M. Andolina, and M. Polini, *Phys. Rev. B* **100**, 115142 (2019).
- [35] D. Rosa, D. Rossini, G. M. Andolina, M. Polini, and M. Carrega, *J. High Energy Phys.* **11** (2020) 067.
- [36] E. McKay, N. A. Rodríguez-Briones, and E. Martín-Martínez, *Phys. Rev. E* **98**, 032132 (2018).
- [37] M. Perarnau-Llobet and R. Uzdin, *New J. Phys.* **21**, 083023 (2019).
- [38] V. P. Patil, Ž. Kos, M. Ravnik, and J. Dunkel, *Phys. Rev. Res.* **2**, 043196 (2020).
- [39] K. V. Hovhannisyán, M. Perarnau-Llobet, M. Huber, and A. Acín, *Phys. Rev. Lett.* **111**, 240401 (2013).
- [40] A. Crescente, D. Ferraro, M. Carrega, and M. Sassetti, *Entropy* **25**, 758 (2023).
- [41] C. K. Hu, J. Qiu, P. J. P. Souza, J. Yuan, Y. Zhou, L. Zhang, J. Chu, X. Pan, L. Hu, J. Li *et al.*, *Quantum Sci. Technol.* **7**, 045018 (2022).
- [42] G. Zhu, Y. Chen, Y. Hasegawa, and P. Xue, *Phys. Rev. Lett.* **131**, 240401 (2023).
- [43] J. Q. Quach, K. E. McGhee, L. Ganzer, D. M. Rouse, B. W. Lovett, E. M. Gauger, J. Keeling, G. Cerullo, D. G. Lidzey, and T. Virgili, *Sci. Adv.* **8**, eabk3160 (2022).
- [44] R. R. Rodríguez, B. Ahmadi, P. Mazurek, S. Barzanjeh, R. Alicki, and P. Horodecki, *Phys. Rev. A* **107**, 042419 (2023).
- [45] C. A. Downing and M. S. Ukharty, *Phys. Rev. A* **109**, 052206 (2024).
- [46] D. Ferraro, M. Campisi, G. M. Andolina, V. Pellegrini, and M. Polini, *Phys. Rev. Lett.* **120**, 117702 (2018).
- [47] H.-L. Shi, S. Ding, Q.-K. Wan, X.-H. Wang, and W.-L. Yang, *Phys. Rev. Lett.* **129**, 130602 (2022).
- [48] M. B. Arjmandi, A. Shokri, E. Faizi, and H. Mohammadi, *Phys. Rev. A* **106**, 062609 (2022).
- [49] J.-W. Zhang, B. Wang, W.-F. Yuan, J.-C. Li, J.-T. Bu, G.-Y. Ding, W.-Q. Ding, L. Chen, F. Zhou, and M. Feng, *Phys. Rev. Lett.* **132**, 180401 (2024).
- [50] F. T. Tabesh, F. H. Kamin, and S. Salimi, *Phys. Rev. A* **102**, 052223 (2020).
- [51] F. H. Kamin, F. T. Tabesh, S. Salimi, F. Kheirandish, and A. C. Santos, *New J. Phys.* **22**, 083007 (2020).
- [52] G. Francica, J. Goold, F. Plastina, and M. Paternostro, *npj Quantum Inf.* **3**, 12 (2017).
- [53] M. Perarnau-Llobet, K. V. Hovhannisyán, M. Huber, P. Skrzypczyk, J. Tura, and A. Acín, *Phys. Rev. E* **92**, 042147 (2015).
- [54] W. K. Wootters, *Phys. Rev. Lett.* **80**, 2245 (1998).
- [55] A. Osterloh, L. Amico, G. Falci, and R. Fazio, *Nature (London)* **416**, 608 (2002).
- [56] C. H. Bennett, D. P. DiVincenzo, J. A. Smolin, and W. K. Wootters, *Phys. Rev. A* **54**, 3824 (1996).
- [57] S. A. Hill and W. K. Wootters, *Phys. Rev. Lett.* **78**, 5022 (1997).
- [58] S. M. Hashemi Rafsanjani, M. Huber, C. J. Broadbent, and J. H. Eberly, *Phys. Rev. A* **86**, 062303 (2012).
- [59] J. Majer, J. M. Chow, J. M. Gambetta, J. Koch, B. R. Johnson, J. A. Schreier, L. Frunzio, D. I. Schuster, A. A. Houck, A. Wallraff *et al.*, *Nature (London)* **449**, 443 (2007).
- [60] G. Wendin, *Rep. Prog. Phys.* **80**, 106001 (2017).
- [61] Z.-L. Xiang, S. Ashhab, J. Q. You, and F. Nori, *Rev. Mod. Phys.* **85**, 623 (2013).
- [62] A. Blais, A. L. Grimsmo, S. M. Girvin, and A. Wallraff, *Rev. Mod. Phys.* **93**, 025005 (2021).
- [63] I. Siddiqi, R. Vijay, F. Pierre, C. M. Wilson, M. Metcalfe, C. Rigetti, L. Frunzio, and M. H. Devoret, *Phys. Rev. Lett.* **93**, 207002 (2004).
- [64] A. Eddins, J. M. Kreikebaum, D. M. Toyli, E. M. Levenson-Falk, A. Dove, W. P. Livingston, B. A. Levitan, L. C. G. Govia, A. A. Clerk, and I. Siddiqi, *Phys. Rev. X* **9**, 011004 (2019).